Research Article

Hydrodynamics of a Free Floating Vertical Axisymmetric Oscillating Water Column Device

S. A. Mavrakos and D. N. Konispoliatis

Laboratory for Floating Structures, Mooring Systems and Division of Marine Structures,
School of Naval Architecture and Marine Engineering, National Technical University of Athens,
9 Heroon Polytechniou Avenue, GR 157-73 Athens, Greece

Correspondence should be addressed to S. A. Mavrakos, mavrakos@naval.ntua.gr

This paper aims at presenting a general formulation of the hydrodynamic problem of a floating or restrained oscillating water column device. Three types of first-order boundary value problems are investigated in order to calculate the velocity potential of the flow field around the device. The horizontal and vertical exciting wave forces, the rolling moment, the hydrodynamic parameters, the volume flows, and the drift forces are obtained in order to find the loads on the structure. The efficiency rate of the device is calculated in connection with the absorbed power and the capture length of energy absorption. Finally, the resulting wave motion inside and outside the device and the inner air pressure are examined.

1. Introduction

In the last years considerable efforts and advances have been made worldwide in exploiting the energy of ocean waves due to the rise of the world's energy consumption and the requirement for "green" energy production. Among several classes of designs proposed for the wave energy conversion, the oscillating water column device (OWC) has received considerable theoretical attention. The OWC device is a partially submerged, hollow structure open to the seabed below the water line. The vertical motion of the sea surface alternatively pressurizes and depressurizes the air inside the structure generating a reciprocating flow through a self-rectifying turbine which is installed beneath the roof of the device. Full sized fixed and floating prototypes were built in Norway (in Toftestallen, near Bergen, 1985), Japan (Sakata, 1990), India (Vizhinjam, near Trivandrum, Kerala State, 1990), Portugal (Pico, Azores, 1999), UK (Scotland, 2000), and Japan (1998) [1, 2].

A nearshore or onshore OWC device was analysed among others by McCormick [3, 4], Evans [5], Sarmento et al. [6], Evans and Porter [7], and Kokkinowrachos et al. [8], for 2D and 3D geometries of OWC devices with infinitesimal wall thickness. Hydrodynamic analysis on a freely floating oscillating water column device could benefit from previous worldwide studies on the dynamics of ships in wavy seas. The first theoretical analysis of a floating oscillating water column device has been presented by Masuda [9]. He developed a navigation buoy powered by wave energy, and equipped with an air turbine, while later promoted the construction of a floating barge (80 m × 12 m), named Kaimei, which housed several OWCs equipped with different types of air turbines [10]. Recently, Martins-Rivas and Mei [11] presented an analysis on an OWC device mounded at the tip of a breakwater with infinitesimal wall thickness and Falcão et al. [12] studied the dynamics of an OWC spar buoy.

In the present contribution, a vertical axisymmetric oscillating water column device with finite wall thickness is examined that is free to move in finite depth waters. Numerical results are given from the solution of three boundary value problems, namely, the diffraction problem (body fixed in waves, atmospheric pressure on the OWC), the radiation problem resulting from the forced oscillations of the body in otherwise still water, also under atmospheric conditions above the OWC, and the radiation problem resulting from an oscillating pressure head acting on the inner free surface of the OWC. Particularly, numerically evaluated linear exciting wave forces in the horizontal and vertical directions along with the volume flow, the added mass and wave damping coefficients are calculated for the freely floating device. In view of evaluating the rigid body motions of the device, the motion equations are solved in the frequency domain, for various values of turbine parameters related to the pressure drop inside the oscillating chamber. The developed method is based on matched axisymmetric eigenfunction expansions of the velocity potential in properly defined ring-shaped fluid regions around the device and could be considered as an extension of the methods employed by Miles and Gilbert [13], Garrett [14], and Yeung [15] as far as a circular dock is concerned, by Mavrakos [16, 17] for bottomless cylinders, by Kokkinowrachos et al. [18] for the hydrodynamic analysis (diffraction and radiation problems) of arbitrary shaped vertical bodies of revolution. In particular, the method extends the formulation given by Evans and Porter [7] to account for finite wall thickness of the vertical bottomless cylindrical chamber and the related 2D formulation by Kokkinowrachos et al. [8] to the case of freely moved vertical cylindrical ducts. The first-order numerical results for the oscillating water column device are supplemented with corresponding ones concerning the wave elevation around the OWC configuration. Finally, the paper investigates the time-independent part of the second-order wave forces (drift forces) on the device's wall and the absorbed wave energy and capture length from the OWC device. Among several types of self-rectifying air turbines that have been developed to equip OWCs [19, 20], it is assumed that a "Wells" turbine, named after its inventor, is installed beneath the roof of the device.

2. Formulation of the Hydrodynamic Problem

We consider a freely floating vertical axisymmetric cylindrical OWC device (Figure 1) of internal and external radius b and a, respectively, excited by regular waves of amplitude $H/2$, frequency ω, and wave number k in constant water depth, d. The draught of the device's chamber is $(d - h)$. We assume small amplitude waves and motions and inviscid incompressible irrotational flow. Cylindrical coordinates (r, θ, z) are introduced with the
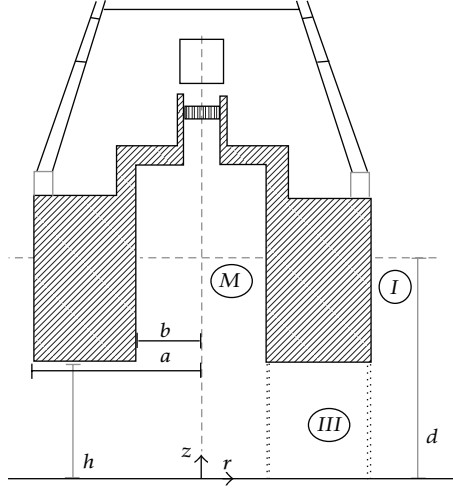
Figure 1: Typical floating oscillating water column device with finite wall thickness. Ring elements definition.

vertical axis Oz directed upwards and origin at the sea bed. For the OWC device, we expect the internal free surface of the device to be subjected to an oscillating pressure head P_{in} with $P_{in}(t) = \text{Re}[p_{in0} \cdot e^{-i\omega t}]$, having the same frequency, ω, as the incident wave.

The time harmonic complex velocity potential of the flow field around the structure can be expressed as

$$\Phi(r, \theta, z; t) = \text{Re}\left[\phi(r, \theta, z) \cdot e^{-i\omega t}\right]. \tag{2.1}$$

We decompose the above velocity potential as

$$\phi = \phi_0 + \phi_7 + \sum_{j=1,3,5} \dot{x}_{j0} \cdot \phi_j + \phi_P. \tag{2.2}$$

Here, ϕ_0 is the velocity potential of the undisturbed incident harmonic wave; ϕ_7 is the scattered potential for the body fixed in the waves with the duct open to the atmosphere, that is, for a pressure in the chamber equal to the atmospheric one; ϕ_j, $(j = 1, 3, 5)$, is the radiation potential resulting from the forced body motion in the jth mode of motion with unit velocity amplitude $\dot{x}_{j0}$ with the duct open to the atmosphere; ϕ_P is the radiation potential resulting from the oscillating pressure head, P_{in}, in the chamber for the body fixed in otherwise calm water.

The undisturbed incident wave potential, ϕ_0, can be expressed in cylindrical coordinates as [21]

$$\phi_0(r, \theta, z) = -i\omega\left(\frac{H}{2}\right) \sum_{m=0}^{\infty} \varepsilon_m i^m \Psi_{0,m}(r, z) \cos(m\theta), \tag{2.3}$$

where

$$\frac{1}{d}\Psi_{0,m}(r,z) = \frac{Z_0(z)}{dZ'_0(d)}J_m(kr).$$

(2.4)

Here, J_m is the mth order Bessel function of the first kind, ε_m is the Neumann's symbol defined as $\varepsilon_0 = 1$ and $\varepsilon_m = 2$ for $m \geq 1$ and $Z_0(z)$:

$$Z_0(z) = \left[\frac{1}{2}\left[1 + \frac{\sinh(2kd)}{2kd}\right]\right]^{-1/2}\cosh(kz),$$

(2.5)

with $Z'_0(d)$ being its derivative at $z = d$. Frequency ω and wave number k are related by the dispersion equation:

$$\omega^2 = k \cdot g \cdot \tanh(kd).$$

(2.6)

The diffracted potential, ϕ_D, around the restrained structure is described by the velocity potential:

$$\phi_D = \phi_0 + \phi_7.$$

(2.7)

In accordance to (2.3) the diffracted velocity potential of the flow field around the OWC device can be written in the form:

$$\phi_D(r,\theta,z) = -i\omega\left(\frac{H}{2}\right)\sum_{m=0}^{\infty}\varepsilon_m i^m\Psi_{D,m}(r,z)\cos(m\theta).$$

(2.8)

The fluid flow caused by the forced oscillation of a vertical axisymmetric body in otherwise still water is symmetric about the plane $\theta = 0$ and antisymmetric about plane $\theta = \pi/2$ for surge, $(j = 1)$, and pitch, $(j = 5)$, whereas it is symmetric about both these planes for heave, $(j = 3)$. Thus the corresponding velocity potentials for these modes of motion can be expressed as

$$\phi_1(r,\theta,z) = \Psi_{1,1}(r,z)\cos(\theta),$$

(2.9)

$$\phi_3(r,\theta,z) = \Psi_{3,0}(r,z),$$

(2.10)

$$\phi_5(r,\theta,z) = \Psi_{5,1}(r,z)\cos(\theta).$$

(2.11)

As for the radiation potential ϕ_P, we note that due to the high sound speed in air, the low frequency of sea waves, and the relatively small per unit volume air kinetic energy, the air pressure can be assumed to be spatially uniform throughout the axisymmetric chamber [11]. Thus, since the forcing of the internal free surface is independent of θ, the radiation potential

ϕ_P will be axially symmetric and so it will include only the $m = 0$ angular mode, that is, it holds:

$$\phi_P(r, \theta, z) = \frac{p_{in0}}{i\omega\rho} \Psi_{P,0}(r, z). \tag{2.12}$$

In the functions $\Psi_{j,m}$ of (2.8)–(2.12) the first subscript $j = D, 1, 3, 5, P$ denotes the respective boundary value problem each time considered, whereas the second one indicates the value of m which must be taken into account for the solution of the corresponding problem. Thus the functions $\Psi_{D,m}$, $(m = 0, 1, 2, \ldots)$, $\Psi_{1,1}$, $\Psi_{3,0}$, $\Psi_{5,1}$, and $\Psi_{P,0}$ remain the principal unknowns of the problem.

The velocity potentials ϕ_j, $(j = D, 1, 3, 5, P)$, have to satisfy the Laplace equation

$$\nabla^2 \phi_j = \frac{\partial^2 \phi_j}{\partial r^2} + \frac{1}{r}\frac{\partial \phi_j}{\partial r} + \frac{1}{r^2}\frac{\partial^2 \phi_j}{\partial \theta^2} + \frac{\partial^2 \phi_j}{\partial z^2} = 0 \tag{2.13}$$

within the entire fluid domain, the linearized boundary condition at the outer and inner free sea surface $(z = d)$, that is,

$$\omega^2 \phi_j - g\frac{\partial \phi_j}{\partial z} = \begin{cases} 0 & \text{for } r \geq a, \ j = D, 1, 3, 5, P, \\ 0 & \text{for } 0 \leq r \leq b, \ j = D, 1, 3, 5, \\ -\dfrac{i\omega}{\rho}p_{in0} & \text{for } 0 \leq r \leq b, \ j = P, \end{cases} \tag{2.14}$$

and the zero normal velocity on the sea bed, that is,

$$\left[\frac{\partial \phi_j(r, \theta, z)}{dz}\right]_{z=0} = 0, \quad j = 1, 3, 5, 7, P. \tag{2.15}$$

Furthermore, the velocity potentials ϕ_j, $(j = D, 1, 3, 5, P)$, have to fulfill following kinematic conditions on the mean device's wetted surface S_0:

$$\frac{\partial \phi_i}{\partial \vec{n}} = 0, \quad i = D, P, \qquad \frac{\partial \phi_j}{\partial \vec{n}} = n_j, \quad j = 1, 3, 5, \tag{2.16}$$

where in (2.16) $\partial(\ )/\partial\vec{n}$ denotes the derivative in the direction of the outward unit normal vector $\vec{n}$, to the wetted surface S_0 of the device and n_j are its generalized components defined as $(n_1, n_2, n_3) = \vec{n}$ and $(n_4, n_5, n_6) = \vec{r} \times \vec{n}$, where $\vec{r}$ is the position vector with respect to the origin of the coordinate system.

We also require the scattered potential to satisfy an appropriate radiation condition as $r \to \infty$, which has the form:

$$\lim_{r\to\infty} \sqrt{kr}\left(\frac{\partial \phi_j}{\partial r} - ik\phi_j\right) = 0, \quad j = 1, 3, 5, 7, P. \tag{2.17}$$

Moreover, the velocity potentials, ϕ_j, and their derivatives, $\partial\phi_j/\partial r$, $(j = D, 1, 3, 5, P)$ must be continuous at the vertical boundaries of neighbouring fluid regions (Figure 1). This results in:

$$\Psi_{j,m}^{III}(b, z) = \Psi_{j,m}^{M}(b, z) \quad \text{for } 0 \leq z \leq h, \tag{2.18}$$

$$\left.\frac{\partial\Psi_{j,m}^{III}}{\partial r}\right|_{r=b} = \left.\frac{\partial\Psi_{j,m}^{M}}{\partial r}\right|_{r=b} \quad \text{for } 0 \leq z \leq h, \tag{2.19}$$

$$\Psi_{j,m}^{I}(a, z) = \Psi_{j,m}^{III}(a, z) \quad \text{for } 0 \leq z \leq h, \tag{2.20}$$

$$\left.\frac{\partial\Psi_{j,m}^{I}}{\partial r}\right|_{r=a} = \left.\frac{\partial\Psi_{j,m}^{III}}{\partial r}\right|_{r=a} \quad \text{for } 0 \leq z \leq h. \tag{2.21}$$

The superscripts I, III, M imply quantities corresponding to respective types of ring elements.

Starting with the method of separation of variables for the Laplace differential equation, appropriate expressions for the velocity potentials, $\Psi_{j,m}^{i}$, in each fluid domain (Figure 1; $i = I, III, M$) can be established [14, 16, 21]. These expressions satisfy the corresponding conditions at the horizontal boundaries of each fluid region and, in addition, the radiation condition at infinity in the outer fluid domain. As a result, the velocity potentials in each fluid domain fulfil a priori the kinematical boundary conditions at the horizontal walls of the device, the linearized condition at the free surface, the kinematical one on the sea bed, and the radiation condition at infinity.

3. Diffraction and Radiation Potentials for Various Fluid Regions

For each type of fluid domain the following expressions for the functions $\Psi_{j,m}^{i}$ involved in (2.8)–(2.12) can be derived.

(a) *Infinite Fluid Domain. Type I* $(r \geq a, \ 0 \leq z \leq d)$

One has

$$\frac{1}{\delta_j}\Psi_{j,m}^{I}(r, z) = g_{jm}^{I}(r, z) + F_{j,m,0}^{I}\frac{H_m(kr)}{H_m(ka)}Z_0(z) + \sum_{i=1}^{\infty}F_{j,m,i}^{I}\frac{K_m(a_ir)}{K_m(a_ia)}Z_i(z), \tag{3.1}$$

where $j = D, 1, 3, 5, P$ and

$$g_{Dm}^{I}(r, z) = \left\{J_m(kr) - \frac{J_m(ka)}{H_m(ka)}H_m(kr)\right\}\frac{Z_0(z)}{dZ_0'(d)},$$

$$g_{11}^{I}(r, z) = g_{30}^{I}(r, z) = g_{51}^{I}(r, z) = g_{P0}^{I}(r, z) = 0, \tag{3.2}$$

$$\delta_D = \delta_1 = \delta_3 = d, \qquad \delta_5 = d^2, \qquad \delta_P = 1.$$

H_m and K_m are the mth order Hankel function of the first kind and the modified Bessel function of the second type, respectively, and $F^I_{j,m,i}$ are unknown Fourier coefficients to be determined by the solution procedure. Moreover, $Z_i(z)$ are orthonormal functions in $[0, d]$ defined by (2.5) for $i = 0$ and by

$$Z_i(z) = \left[\frac{1}{2}\left[1 + \frac{\sin(2a_i d)}{2a_i d}\right]\right]^{-1/2} \cos(a_i z), \quad i \geq 1. \tag{3.3}$$

The eigenvalues α_i are roots of the transcendental equation:

$$\omega^2 + g \cdot a_i \cdot \tan(a_i d) = 0, \tag{3.4}$$

which possesses one imaginary, $a_0 = -ik$, $k > 0$, and infinite number of real roots. Substituting the value of a_0 in (3.3) and (3.4), (2.5) and (2.6) can directly be obtained.

(b) *Fluid Region of Type III* ($b \leq r \leq a$, $0 \leq z \leq h$)

One has

$$\frac{1}{\delta_j} \Psi^{III}_{j,m}(r, z) = g^{III}_{jm}(r, z) + \sum_{q=0}^{\infty} \varepsilon_q \left[R^{III}_{mq}(r) F^{III}_{j,m,q} + R^{*III}_{mq}(r) F^{*III}_{j,m,q}\right] \cos\left(\frac{q\pi z}{h}\right), \tag{3.5}$$

where $j = D, 1, 3, 5, P$ and

$$g^{III}_{Dm}(r, z) = g^{III}_{11}(r, z) = g^{III}_{P0}(r, z) = 0, \tag{3.6}$$

$$g^{III}_{30}(r, z) = \frac{z^2 - (1/2)r^2}{2hd}, \qquad g^{III}_{51}(r, z) = \frac{-r\left[z^2 - (1/4)r^2\right]}{2hd^2}, \tag{3.7}$$

$$R^{III}_{mq}(r) = \frac{K_m(q\pi b/h)I_m(q\pi r/h) - I_m(q\pi b/h)K_m(q\pi r/h)}{I_m(q\pi a/h)K_m(q\pi b/h) - I_m(q\pi b/h)K_m(q\pi a/h)}, \quad m, q \neq 0,$$

$$R^{III}_{m0}(r) = \frac{(r/b)^m - (b/r)^m}{(a/b)^m - (b/a)^m}, \quad m \neq 0, q = 0, \qquad R^{III}_{00}(r) = \frac{\ln(r/b)}{\ln(a/b)}, \quad m, q = 0, \tag{3.8}$$

$$R^{*III}_{mq}(r) = \frac{I_m(q\pi a/h)K_m(q\pi r/h) - K_m(q\pi a/h)I_m(q\pi r/h)}{I_m(q\pi a/h)K_m(q\pi b/h) - I_m(q\pi b/h)K_m(q\pi a/h)}, \quad m, q \neq 0,$$

$$R^{*III}_{m0}(r) = \frac{(a/r)^m - (r/a)^m}{(a/b)^m - (b/a)^m}, \quad m \neq 0, \ q = 0, \qquad R^{*III}_{00}(r) = \frac{\ln(a/r)}{\ln(a/b)}, \quad m, q = 0. \tag{3.9}$$

I_m is the mth order modified Bessel function of the first kind and $F^{III}_{j,m,q}$, $F^{*III}_{j,m,q}$ are Fourier coefficients to be determined by the solution procedure. The functions $g^{III}_{jm}(r, z)$ in (3.6) and (3.7) above represent harmonic particular solutions for the surge, heave, and pitch modes of motion [15, 17, 18] that fulfill the inhomogeneous boundary condition (2.16) for the heave and pitch motions at the bottom surface of the OWC device.

(c) *Interior Fluid Region of Type M* ($r \leq b,\ 0 \leq z \leq d$)

One has

$$\frac{1}{\delta_j}\Psi_{j,m}^M(r,z) = g_{jm}^M(r,z) + \sum_{i=0}^{\infty} F_{j,m,i}^M \frac{I_m(a_i r)}{I_m(a_i b)} Z_i(z),\qquad(3.10)$$

where $j = D, 1, 3, 5, P$ and

$$g_{Dm}^M(r,z) = g_{11}^M(r,z) = g_{30}^M(r,z) = g_{51}^M(r,z) = 0,\qquad g_{P0}^M(r,z) = 1.\qquad(3.11)$$

Here, the orthonormal functions $Z_i(z)$ are defined by (2.5) and (3.3), for $i = 0$ and $i \geq 1$, respectively, and a_i are given by (3.4). Moreover, $F_{j,m,i}^M$ are unknown Fourier coefficients in the Mth fluid region. The function $g_{P0}^M(r,z)$ has been introduced in (3.10) in order for the inhomogeneous boundary condition on the water surface in the interior fluid region, (2.14) to be fulfilled in the case of the pressure radiation problem.

   The solutions for the potential functions $\Psi_{j,m}^i$, ($i = I, III, M$ and $j = D, 1, 3, 5, P$), expressed through (3.1), (3.5), and (3.10), are constructed in such a way that the conditions at all the horizontal boundaries of each fluid region and, in addition, the radiation condition at infinity in the outer fluid domain are a priori satisfied. Moreover, the potential functions $\Psi_{j,m}^i$ have been constructed in such a way that their homogeneous parts can be reduced to simple Fourier series at the vertical boundaries of the various fluid regions, that is, $r = a, b$. This feature of the velocity potential representations facilitates essentially the solution procedure. The kinematic conditions at the body's vertical walls, (2.16), as well as the requirement for continuity of the potential and its radial derivative, (2.18)–(2.21), at the vertical boundaries of neighboring fluid domains remain to be fulfilled. Expressing these conditions, the system of equations for the unknown Fourier coefficients is obtained. Once these coefficients have been calculated, the functions $\Psi_{j,m}^i$ and hence the velocity potential for all fluid regions can be evaluated. Methods for the solution of the diffraction and the radiation problem originated from the forced body motion in otherwise still water have been extensively reported in previous works [16, 17] and, so, they are no further elaborated here. Only the solution procedure for the pressure radiation problem will be outlined in the next section.

4. Solution Procedure for the Pressure Radiation Problem

The condition for continuity of the potential function at $r = b$ and $r = a$ is expressed by (2.18) and (2.20), respectively. Multiplying both sides of equations by $(1/h)\cos(\nu\pi z/h)$ and integrating over their region of validity, that is, $0 \leq z \leq h$ the following set of equations can be obtained:

$$\sum_{q=0}^{\infty} F_{P,0,q}^{*III} = Q_{P,0,q}^* + \sum_{i=0}^{\infty} L_{q,i} F_{P,0,i}^M,\quad \text{for } 0 \leq z \leq h,\ r = b,\qquad(4.1)$$

$$\sum_{q=0}^{\infty} F_{P,0,q}^{III} = \sum_{i=0}^{\infty} L_{q,i} F_{P,0,i}^I,\quad \text{for } 0 \leq z \leq h,\ r = a,\qquad(4.2)$$

where

$$L_{q,i} = \frac{1}{h} \int_0^h Z_i(z) \cos\left(\frac{q\pi z}{h}\right) dz, \tag{4.3}$$

$$Q_{P,0,q}^* = \frac{1}{h} \int_0^h g_{P0}^M(b,z) \cos\left(\frac{q\pi z}{h}\right) dz, \tag{4.4}$$

are defined in Appendix A.

Now, the condition for the continuity of the first derivative of the potential at $r = b$ and $r = a$ as expressed by (2.19) and (2.21), respectively, as well as the kinematic condition on the vertical boundaries of the device as described by (2.16) must be fulfilled too. Multiplying both sides of (2.19), (2.21), and (2.16) with the weight function $(1/d)Z_\mu(z)$, integrating over the region of their validity, that is, $h \le z \le d$ and $0 \le z \le d$, respectively, and adding the resulting expressions, the following set of equations is obtained:

$$\sum_{i=0}^{\infty} F_{P,0,i}^M A_{0,i}^M = \frac{h}{d} \sum_{q=0}^{\infty} \varepsilon_q L_{q,i} D_{0q}^{III} F_{P,0,q}^{III} + \frac{h}{d} \sum_{q=0}^{\infty} \varepsilon_q L_{q,i} D_{0q}^{*III} F_{P,0,q}^{*III}, \quad \text{at } r = b, \tag{4.5}$$

$$\sum_{i=0}^{\infty} F_{P,0,i}^I A_{0,i}^I = \frac{h}{d} \sum_{q=0}^{\infty} \varepsilon_q L_{q,i} \left(A_{0q}^{III} F_{P,0,q}^{III} + A_{0q}^{*III} F_{P,0,q}^{*III} \right), \quad \text{at } r = a, \tag{4.6}$$

where

$$A_{0,i}^M = a_i b \left.\frac{\partial I_0(a_i r)}{\partial r}\right|_{r=b} \frac{1}{I_0(a_i b)}, \qquad A_{0,i}^I = a_i a \left.\frac{\partial K_0(a_i r)}{\partial r}\right|_{r=a} \frac{1}{K_0(a_i a)}, \tag{4.7}$$

$$D_{0q}^{III} = b \left.\frac{\partial R_q^{III}}{\partial r}\right|_{r=b}, \qquad D_{0q}^{*III} = b \left.\frac{\partial R_{0q}^{*III}}{\partial r}\right|_{r=b}, \qquad A_{0q}^{III} = a \left.\frac{\partial R_{0q}^{III}}{\partial r}\right|_{r=a}, \qquad A_{0q}^{*III} = a \left.\frac{\partial R_{0q}^{*III}}{\partial r}\right|_{r=a}, \tag{4.8}$$

and R_{0q}^{III}, R_{0q}^{*III} are defined in (3.8) and (3.9), respectively. For the numerical implementation of the method, series (3.1), (3.5), and (3.10) expressing the potential in I, III, M fluid region will be truncated after Q, M, and N terms, respectively.

Substituting (4.1) into (4.5) will provide the unknown Fourier coefficients, $F_{P,0,i}^M$, in the M fluid domain in relation with the Fourier coefficients, $F_{P,0,q}^{III}$, in the III fluid domain, in the following matrix form, that is,

$$\left(\left[A_{0,i}^M \right] - \frac{h}{d} \sum_{q=0}^{\infty} \left[L_{i,q}^{M,III} \right] \cdot \left[\varepsilon_q \right] \cdot \left[D_{0q}^{*III} \right] \cdot \left[L_{q,i}^{III,M} \right] \right) \cdot \left\{ F_{P,0,i}^M \right\}$$

$$= \frac{h}{d} \left[L_{i,q}^{M,III} \right] \cdot \left[\varepsilon_q \right] \cdot \left[D_{0q}^{III} \right] \cdot \left\{ F_{P,0,q}^{III} \right\} + \frac{h}{d} \left[L_{i,q}^{M,III} \right] \cdot \left[\varepsilon_q \right] \cdot \left[D_{0q}^{*III} \right] \cdot \left\{ Q_{P,0,q}^* \right\}, \tag{4.9}$$

where, $\{F^M_{P,0,i}\}$ and $\{F^{III}_{P,0,q}\}$ are both complex vectors, the elements of which are the unknown Fourier coefficients in the Mth and IIIth fluid domain, respectively, $[A^M_{0,i}]$ is a $(N \times N)$ diagonal matrix given by (4.7), $[L^{M,III}_{i,q}]$ is a $(N \times M)$ matrix given by (4.3), $[\varepsilon_q]$ is the Neumann's symbol $(M \times M)$ diagonal matrix with $\varepsilon_{11} = 1$ and $\varepsilon_{kk} = 2$ for $k \geq 2$, $[D^{III}_{0q}]$ and $[D^{*III}_{0q}]$ are $(M \times M)$ diagonal matrices defined in (4.8), and $\{Q^*_{P,0,q}\}$ is a column vector $(M \times 1)$ defined in (4.4).

From (4.9) and (4.1), the Fourier coefficients, $F^{III}_{P,0,q}$ and $F^{*III}_{P,0,q}$, in the IIIth fluid domain are connected with the bellow relation:

$$\left\{F^{*III}_{P,0,q}\right\} = \frac{h}{d}\left[L^{III,M}_{q,i}\right] \cdot [G_{i,i}]^{-1} \cdot \left[L^{M,III}_{i,q}\right] \cdot [\varepsilon_q] \cdot \left[D^{III}_{0q}\right] \cdot \left\{F^{III}_{P,0,q}\right\}$$
$$+ \left([I] + \frac{h}{d}\left[L^{III,M}_{q,i}\right] \cdot [G_{i,i}]^{-1} \cdot \left[L^{M,III}_{i,q}\right] \cdot [\varepsilon_q] \cdot \left[D^{*III}_{0q}\right]\right) \cdot \left\{Q^*_{P,0,q}\right\}, \tag{4.10}$$

where $[I]$ is the unit matrix and

$$[G_{i,i}] = \left[A^M_{0,i}\right] - \frac{h}{d}\sum_{q=0}^{\infty}\left[L^{M,III}_{i,q}\right] \cdot [\varepsilon_q] \cdot \left[D^{*III}_{0q}\right] \cdot \left[L^{III,M}_{q,i}\right], \tag{4.11}$$

where, $\{F^{*III}_{P,0,q}\}$ is a complex vector, the elements of which are the unknown Fourier coefficients in the IIIth region.

Substituting (4.2) into (4.6) will provide the unknown Fourier coefficients, $F^I_{P,0,i}$, in the Ith fluid domain in relation with the Fourier coefficients, $F^{III}_{P,0,q}, F^{*III}_{P,0,q}$, in the III fluid domain, in the following matrix form, that is,

$$\left[A^I_{0,i}\right] \cdot \left\{F^I_{P,0,i}\right\} = \frac{h}{d}\left[L^{I,III}_{i,q}\right] \cdot [\varepsilon_q] \cdot \left[A^{III}_{0q}\right] \cdot \left\{F^{III}_{P,0,q}\right\} + \frac{h}{d}\left[L^{I,III}_{i,q}\right] \cdot [\varepsilon_q] \cdot \left[A^{*III}_{0q}\right] \cdot \left\{F^{*III}_{P,0,q}\right\}, \tag{4.12}$$

where, $\{F^I_{P,0,i}\}$ is a complex vector, the elements of which are the unknown Fourier coefficients in the I fluid domain, $[A^I_{0,i}]$ is a $(Q \times Q)$ diagonal matrix given by (4.7), and $[L^{I,III}_{i,q}]$ is a $(Q \times M)$ matrix given by (4.3).

After determining the Fourier coefficients for the pressure radiation problem in all fluid domains, by solving the system equations (4.9), (4.10), and (4.12), and the Fourier coefficients for the diffraction and motion radiation problem from previous work [16, 17] and substituting them into (3.1), (3.5), (3.10), the velocity potential of the flow field in each fluid region around the free floating body can be determined.

5. Volume Flow

During the water oscillation inside the chamber the dry air above the free surface is being pushed through a Wells turbine. The volume flow produced by the oscillating internal water surface is denoted by $Q(t) = \text{Re}\{q \cdot e^{-i\omega t}\}$ where

$$q = \iint_{S_i} u_z dS_i = \iint_{S_i} u(r,\theta,z=d)r dr\, d\theta = \iint_{S_i} \frac{\partial \phi}{\partial z} r dr\, d\theta. \tag{5.1}$$

Here u_z denotes the vertical velocity of the water surface, and S_i the cross-sectional area of the inner water surface.

By substituting (2.2) into (5.1) it proves convenient to decompose the total volume flow, q, into three terms associated with the diffraction, q_D, the motion-dependent-, q_R, and the pressure-dependent-radiation problems, q_P, as follows:

$$q = q_D + q_R + q_P. \tag{5.2}$$

Assuming uniform pressure distribution inside the chamber, only the pumping mode for $m = 0$ affects the volumetric oscillations in evaluating q_P. Moreover, by substituting (2.8) into (5.1) it can be shown that only modes with $m = 0$ contribute to q_D. Finally, the volume flow rate due to motion-dependent radiation potentials q_R can be expressed on the basis of the relative displacement between the internal free surface elevation and the motions of the device. Due to the fact that the motions in the horizontal plane (surge) and the pitch mode for a vertical axisymmetric OWC device do not affect the volume of air in its chamber, only the velocity potential due to the vertical displacement x_{30} of the device will contribute to the volume flow rate, that is,

$$q_R = q_3 - \dot{x}_{30} S_i. \tag{5.3}$$

By accounting (5.2), (5.1), and (5.3) it can be obtained that

$$q_D = \iint_{S_i} \frac{\partial}{\partial z}(\phi_0 + \phi_7)\,dS_i,$$

$$q_P = \iint_{S_i} \frac{\partial \phi_P}{\partial z}\,dS_i, \tag{5.4}$$

$$q_R = \iint_{S_i} \dot{x}_{30} \frac{\partial \phi_3}{\partial z}\,dS_i - \dot{x}_{30} S_i.$$

Next, by substituting (3.10) into (2.8), (2.10), and (2.12), we have, respectively,

$$q_D = (-i\omega)2\frac{\omega^2}{g}\frac{H}{2}d\pi b\left(F^M_{D,0,0}\frac{J_1(kb)}{kJ_0(kb)}N_0^{-1/2}\cosh(kd) + \sum_{j=1}^{\infty} F^M_{D,0,j}\frac{I_1(a_j b)}{a_j I_0(a_j b)}N_j^{-1/2}\cos(a_j d) \right), \tag{5.5}$$

$$q_p = (-i\omega)2\frac{p_{in0}}{g\rho}\pi b\left(F^M_{P,0,0}\frac{J_1(kb)}{kJ_0(kb)}N_0^{-1/2}\cosh(kd) + \sum_{j=1}^{\infty} F^M_{P,0,j}\frac{I_1(a_j b)}{a_j I_0(a_j b)}N_j^{-1/2}\cos(a_j d) \right), \tag{5.6}$$

$$q_3 = \dot{x}_{30}2\frac{\omega^2}{g}d\pi b\left(F^M_{3,0,0}\frac{J_1(kb)}{kJ_0(kb)}N_0^{-1/2}\cosh(kd) + \sum_{j=1}^{\infty} F^M_{3,0,j}\frac{I_1(a_j b)}{a_j I_0(a_j b)}N_j^{-1/2}\cos(a_j d) \right). \tag{5.7}$$

The volume flow q_3, induced by the heave mode forced oscillation, can be written as

$$q_3 = (-e_{3P} + iwd_{3P}) \cdot \dot{x}_{30}, \tag{5.8}$$

where e_{3P}, d_{3P} are the real and imaginary part of (5.7). The volume flow associated with the pressure radiation problem q_P, (5.6), can be decomposed into real and imaginary part, f_{PP}, g_{PP}, respectively, as

$$q_P = -(f_{PP} - ig_{PP}) \cdot p_{in0}, \tag{5.9}$$

where g_{PP} is in phase with the flow acceleration and amounts to the added hydrodynamic inertia (i.e., radiation susceptance) and f_{PP} is in phase with the flow velocity amounting to radiation damping (i.e., radiation conductance) [7, 11].

We assume that the Wells turbine is placed in a duct between the chamber and the outer atmosphere and the total volume flow Q is proportional to the chamber air pressure [7, 22]:

$$Q(t) = \Lambda \cdot P_{in}(t), \tag{5.10}$$

Λ representing a pneumatic complex admittance.

The mass flow rate of air though the turbine can be written as [5]

$$\dot{m}(t) = -\frac{d(\rho_{in}(t) \cdot V_{in}(t))}{dt}. \tag{5.11}$$

Here V_{in} is the air chamber volume, ρ_{in} is the air density, which can be related to the atmospheric density ρ_a, by assuming isentropic density-pressure relations, small air density variation and linearization with respect to the pressure [5], that is,

$$\rho_{in}(t) = \rho_a \left[1 + \frac{P_{in}(t)}{\gamma \cdot P_a} \right]. \tag{5.12}$$

whith $\gamma = 1.4$ being the adiabatic constant and P_a the atmospheric pressure. By inserting (5.11), (5.12) into (5.10), the air volume flow rate through the turbine is [5]

$$\frac{\dot{m}}{\rho_a} = Q(t) - \frac{V_0}{\gamma \cdot P_a} \frac{dP_{in}(t)}{dt}, \tag{5.13}$$

where V_0 is the value of V_{in} in undisturbed conditions. The turbine aerodynamic performance can be written in dimensionless form as [23, 24]

$$\Phi = \frac{\dot{m}}{\rho_a N D^3}, \qquad \Psi = \frac{P_{in}}{\rho_a N^2 D^2}, \qquad \Pi = \frac{E}{\rho_a N^3 D^5}, \tag{5.14}$$

where N is the rotational speed (radians per unit time) of turbine blades, E the turbine power output, and D the turbine rotor diameter. It was found [25] that for the Wells turbine:

$$\Phi = K \cdot \Psi, \tag{5.15}$$

where K is constant for a given turbine geometry (independent of turbine size or rotational speed). Substitution of (5.14), (5.15) into (5.13) gives [26]

$$q = \left[\frac{KD}{\rho_a N} + (-i\omega) \frac{V_0}{\gamma P_a} \right] p_{in0}. \tag{5.16}$$

From (5.10) and (5.16):

$$\Lambda = g_T + (-i\omega) \frac{V_0}{\gamma P_a}, \tag{5.17}$$

where $g_T = KD/\rho_a N$.

6. Wave Forces

The various forces on the oscillating water column device can be calculated from the pressure distribution given by the linearised Bernoulli's equation:

$$P(r, \theta, z; t) = -\rho \frac{\partial \Phi}{\partial t} = (-i\omega)\rho\phi \cdot e^{-i\omega t}, \tag{6.1}$$

where ϕ is the velocity potential in each fluid domain I, III, M.

The horizontal wave force, $F_x = \mathrm{Re}(f_x \cdot e^{-i\omega t})$, on the device is given by

$$f_x = f_{x_{\mathrm{Out}}} - f_{x_{\mathrm{In}}} = -i\omega\rho a \int_{z=h}^{z=d} \int_0^{\theta=2\pi} \phi^I \cos\theta d\theta \, dz + i\omega\rho b \int_{z=h}^{z=d} \int_0^{\theta=2\pi} \phi^M \cos\theta d\theta \, dz, \tag{6.2}$$

where $f_{x_{\mathrm{Out}}}$ is the horizontal force on the device's external wall, and $f_{x_{\mathrm{In}}}$ is the horizontal force on the chamber's wall.

The oscillating pressure inside the chamber does not affect the horizontal exciting force on the floating device since the radiation potential includes only the $m = 0$ angular mode. So, the horizontal force on the OWC device is the same as on an open vertical axisymmetric bottomless duct with finite wall thickness [16].

On the contrary, the oscillating pressure inside the chamber does affect the vertical force due to unit internal pressure head, on the floating device. The total vertical force on the OWC device, $F_z = \mathrm{Re}(f_z \cdot e^{-i\omega t})$, is equal to the sum of the vertical wave exciting force, $F_{z_{\mathrm{open}}} = \mathrm{Re}(f_{z_{\mathrm{open}}} \cdot e^{-i\omega t})$, on the device when the duct is open to the atmosphere (diffraction

load) and the vertical force, $F_{z_{\text{close}}} = \text{Re}(f_{z_{\text{close}}} \cdot e^{-i\omega t})$, due to the internal pressure head when the duct is closed:

$$
\begin{aligned}
f_z = f_{z_{\text{open}}} + f_{z_{\text{close}}} &= -i\omega\rho \int_{r=b}^{r=a} \int_0^{\theta=2\pi} \phi^{III}(-1) r d\theta \, dr \\
&= -i\omega\rho \int_{r=b}^{r=a} \int_0^{\theta=2\pi} \left(\phi_D^{III} + \phi_P^{III}\right)(-1) r d\theta \, dr.
\end{aligned}
\tag{6.3}
$$

Substituting (2.8) and (2.12) into (6.3) we extract

$$
\begin{aligned}
\frac{f_{z_{\text{open}}}}{B} = 2kd\tanh(kd) &\left\{ \frac{1}{2} F_{D,0,0}^{III}\left(1 - \frac{1-(b/a)^2}{2\ln(a/b)}\right) - \frac{1}{2} F_{D,0,0}^{*III}\left(\frac{b^2}{a^2} - \frac{1-(b/a)^2}{2\ln(a/b)}\right) \right. \\
&\left. + 2\sum_{n=1}^\infty (-1)^n \left(\frac{h}{n\pi a}\right)^2 \left[F_{D,0,n}^{III}\left(A_{0n}^{III} - D_{0n}^{III}\right) + F_{D,0,n}^{*III}\left(A_{0n}^{*III} - D_{0n}^{*III}\right) \right] \right\},
\end{aligned}
\tag{6.4}
$$

$$
\begin{aligned}
\frac{f_{z_{\text{close}}}}{\pi a^2 p_{\text{in}0}} = 2 &\left\{ \frac{1}{2} F_{P,0,0}^{III}\left(1 - \frac{1-(b/a)^2}{2\ln(a/b)}\right) - \frac{1}{2} F_{P,0,0}^{*III}\left(\frac{b^2}{a^2} - \frac{1-(b/a)^2}{2\ln(a/b)}\right) \right. \\
&\left. + 2\sum_{n=1}^\infty (-1)^n \left(\frac{h}{n\pi a}\right)^2 \left[F_{P,0,n}^{III}\left(A_{0n}^{III} - D_{0n}^{III}\right) + F_{P,0,n}^{*III}\left(A_{0n}^{*III} - D_{0n}^{*III}\right) \right] \right\},
\end{aligned}
\tag{6.5}
$$

where $B = \pi\rho g a^2 (H/2)$ and $F_{D,0,n}^{III}$, $F_{D,0,n}^{*III}$, $F_{P,0,n}^{III}$, and $F_{P,0,n}^{*III}$ are the diffraction and pressure radiation Fourier coefficients for the IIIth type of ring element and A_{0n}^{III}, A_{0n}^{*III}, D_{0n}^{III}, and D_{0n}^{*III} are defined at (4.8).

The vertical force $f_{z_{\text{close}}}$ induced by the oscillating pressure head $p_{\text{in}0}$ is related [8, 22] to the volume flow q_3, induced by the heave mode forced oscillation, (see (5.8)). The above force, $f_{z_{\text{close}}}$, can be written as

$$
f_{z_{\text{close}}} = (-e_{P3} + i\omega d_{P3}) p_{\text{in}0} = (e_{3P} - i\omega d_{3P}) p_{\text{in}0},
\tag{6.6}
$$

where e_{3P}, d_{3P} are the real and imaginary part of (6.5)

The moment on the device about a horizontal axis lying at an arbitrary distance $z = e$ from the sea bed is the real part of $M \cdot e^{-i\omega t}$, where M is made up of M_s and M_b arising from the pressure distribution on the device's vertical walls and on its bottom, respectively, [16]:

$$
\begin{aligned}
M_s &= -i\omega\rho a \int_{z=h}^{z=d} \int_0^{\theta=2\pi} \phi^I (z-e)\cos\theta \, d\theta \, dz + i\omega\rho b \int_{z=h}^{z=d} \int_0^{\theta=2\pi} \phi^M (z-e)\cos\theta \, d\theta \, dz, \\
M_b &= -i\omega\rho \int_{r=b}^{r=a} \int_0^{\theta=2\pi} \phi^{III}(-1) r^2 d\theta \, dr = -i\omega\rho \int_{r=b}^{r=a} \int_0^{\theta=2\pi} \left(\phi_D^{III} + \phi_P^{III}\right)(-1) r^2 d\theta \, dr.
\end{aligned}
\tag{6.7}
$$

7. Added Mass and Damping Coefficients

The hydrodynamic reaction forces and pitching moment $F_{i,j}$ acting on the oscillating water column device in the ith direction due to its sinusoidal motion with frequency ω and unit amplitude in the jth direction can be obtained as the real part of $f_{i,j} \cdot e^{-i\omega t}$, from (6.1):

$$f_{i,j} = -\rho\omega^2 \iint_S \Psi_{j,m}(r,z)\cos(m\theta)n_i \, dS. \tag{7.1}$$

Herein n_i is defined at (2.16) and $\Psi_{j,m}$ is obtained from (3.1), (3.5), and (3.10) in each fluid domain I, III, M.

The complex force $f_{i,j}$ may be written in the form [27]:

$$f_{ij} = \omega^2 a_{ij} + i\omega b_{ij}, \tag{7.2}$$

where a_{ij} and b_{ij} are the added mass and damping coefficients, respectively, both real and dependent on frequency ω. Substituting the appropriate expressions for $\Psi_{j,m}$ in (7.1) and using (7.2), the relations for nondimensionalized hydrodynamic coefficients can be found [17].

8. Motion and Air Pressure Calculation

Assuming that the waves and the device oscillations are described by small amplitude motions, the hydrodynamic problem is well characterized by a linear approach. The 6 degrees of freedom system of motion equations, in the frequency domain, are written as

$$\sum_{j=1}^{6}(m_{kj} + a_{kj})\ddot{x}_j + b_{kj}\dot{x}_j + c_{kj}x_j = F_k(t), \quad k = 1, 2, \ldots, 6, \tag{8.1}$$

where x_j is the 6-degree displacement vector, m_{kj} is the mass matrix, a_{kj} is the frequency-dependent added mass matrix, b_{kj} is the frequency-dependent damping matrix, c_{kj} is the stiffness matrix, and F_k represent the total force (diffraction and pressure induced radiation) on the device.

Under the assumption of symmetrical mass distribution, a vertical body of revolution performs under the action of a regular incident wave three degrees of freedom motion, that is, two translations (x_1: surge, x_3: heave) and one rotation (x_5: pitch). So the (8.1) can be reduced to

$$(m + a_{33})\ddot{x}_{30} + b_{33}\dot{x}_{30} + c_{33}x_{30} = f_3, \tag{8.2}$$

$$(m + a_{11})\ddot{x}_{10} + b_{11}\dot{x}_{10} + c_{11}x_{10} + \left(mX_{g_3}^{(0)} + a_{15}\right)\ddot{x}_{50} + b_{15}\dot{x}_{50} + c_{15}x_{50} = f_1, \tag{8.3}$$

$$(I_{55} + a_{55})\ddot{x}_{50} + b_{55}\dot{x}_{50} + c_{55}x_{50} + \left(mX_{g_3}^{(0)} + a_{51}\right)\ddot{x}_{10} + b_{51}\dot{x}_{10} + c_{51}x_{10} = f_5, \tag{8.4}$$

where

$$c_{11} = c_{15} = c_{51} = 0, \qquad c_{33} = \rho g A_{\text{wp}}, \qquad c_{55} = \rho g V \left(\overline{GM} \right). \qquad (8.5)$$

Also, A_{wp} is the water plane area, $\overline{GM}$ is the metacentric height, $X_{g3}^{(0)}$ is the vertical distance of the centre of gravity from the reference point of motions, and I_{55} is the pitch mass moment of inertia of the device.

Since the oscillating pressure inside the chamber does affect only the vertical exciting force on the floating device, (8.2) can be recast as follows:

$$\left(-i\omega(m + a_{33}) + b_{33} + \frac{i}{\omega} c_{33} \right) \dot{x}_{30} = f_{z_{\text{open}}} + f_{z_{\text{close}}} + f_{MP} \qquad (8.6)$$

with f_{MP} being the force on the chamber's wall due to inner pressure; it is equal to

$$f_{MP} = S_i \cdot p_{\text{in}0}. \qquad (8.7)$$

Combining (8.7), (8.6) we obtain

$$\left(-i\omega(m + a_{33}) + b_{33} + \frac{i}{\omega} c_{33} \right) \dot{x}_{30} + \left(-\frac{f_{z_{\text{close}}}}{p_{\text{in}0}} - \pi b^2 \right) p_{\text{in}0} = f_{z_{\text{open}}}. \qquad (8.8)$$

From (5.16) and (5.2) it is obtained that

$$\left[g_T + (-i\omega) \frac{V_0}{\gamma P_a} \right] p_{\text{in}0} = q_D + q_R + q_P \qquad (8.9)$$

which in turn by considering (5.3) is reduced to

$$\left[-\frac{q_3}{\dot{x}_{30}} + \pi b^2 \right] \dot{x}_{30} + \left[g_T + (-i\omega) \frac{V_0}{\gamma P_a} - \frac{q_P}{p_{\text{in}0}} \right] p_{\text{in}0} = q_D. \qquad (8.10)$$

Solving the system of (8.3), (8.4), (8.8), and (8.10), we calculate the unknown motion components of the device $x_{j0} \; j = 1, 3, 5$ and the internal chamber's pressure $p_{\text{in}0}$. When the body is considered restrained in the waves, the air chamber pressure is deduced from (8.10) for $\dot{x}_{30} = 0$.

9. Wave Runup

The free surface elevation outside and inside the device is given by the linearized boundary condition at the outer and inner free sea surface. It holds:

$$Z(r,\theta,d;t) = \text{Re}\left\{\zeta(r,\theta,d)\cdot e^{-i\omega t}\right\} = \text{Re}\left\{\left(\frac{i\omega}{g}\varphi^I(r,\theta,d)\right)(\cos(\omega t) - i\sin(\omega t))\right\}, \quad (9.1)$$

$$Z(r,\theta,d;t) = \text{Re}\left\{\zeta(r,\theta,d)e^{-i\omega t}\right\} = \text{Re}\left\{\left(\frac{i\omega}{g}\varphi^M(r,\theta,d) - \frac{p_{in0}}{\rho g}\right)(\cos(\omega t) - i\sin(\omega t))\right\}, \quad (9.2)$$

for the outer and inner fluid domains, respectively.

10. Drift Forces

The time-independent part of the second-order wave forces (drift forces) on the floating OWC device, has been evaluated using the direct integration of all pressure terms contributing to second-order loads components over the instantaneous body's wetted surface. It holds [28]:

$$\overline{F_x}^T = -\int_{WL}\frac{1}{2}\cdot\rho\cdot g\cdot\overline{\zeta_r^2}^T n_x d\ell + m\cdot R\cdot\overline{\ddot{X_g}}^T + \iint_{S_0}\frac{1}{2}\cdot\rho\cdot\overline{|\nabla\Phi|^2}^T n_x dS_0 + \iint_{S_0}\rho\cdot\overline{\overline{X}\cdot\nabla\Phi_t}^T n_x dS_0, \quad (10.1)$$

$$\overline{F_z}^T = m\cdot R\cdot\overline{\ddot{X_g}}^T + \iint_{S_0}\frac{1}{2}\cdot\rho\cdot\overline{|\nabla\Phi|^2}^T n_z dS_0 + \iint_{S_0}\rho\cdot\overline{\overline{X}\cdot\nabla\Phi_t}^T n_z dS_0, \quad (10.2)$$

where m is the device's mass, R is the transformation matrix, containing only first-order angular displacement (see, Appendix B), $\ddot{X_g}$ is the acceleration matrix of the body's centre of gravity (see, Appendix B), ρ is the water density, g is the acceleration due to gravity, ζ_r is the relative wave height (see, Appendix B), Φ is the time harmonic complex velocity potential of the flow field around the structure, and $\overline{X}$ is the displacement vector of a point on the device (see, Appendix B).

11. Absorbed Power

The time-averaged power absorbed by the device from the waves, P_{out}, is obtained from [11]

$$P_{out} = \frac{1}{2}\text{Re}\left[\Lambda\cdot|p_{in0}|^2\right], \quad (11.1)$$

where Λ is the turbine's pneumatic admittance, (5.17). By inserting (5.2), (5.16), and (5.17), into (11.1), we obtain

$$P_{out} = \frac{KD}{2\rho_a N}|p_{in0}|^2 = \frac{KD}{2\rho_a N}\frac{\text{Re}\left[(q_D + q_R)\cdot(\overline{q_D} + \overline{q_R})\right]}{(f_{PP} + KD/\rho_a N)^2 + (\omega V_0/\gamma P_a + g_{PP})^2}. \quad (11.2)$$

Alternatively, (11.1) can be expressed as:

$$P_{\text{out}} = \frac{1}{2} \operatorname{Re}\left[(q_D + q_R)\overline{p_{\text{in}0}}\right] - \frac{1}{2}f_{PP}\left|p_{\text{in}0}\right|^2 = \frac{\left|q_D + q_R\right|^2}{8 \cdot f_{PP}} - \frac{f_{PP}}{2}\left|p_{\text{in}0} - \frac{q_D + q_R}{2 \cdot f_{PP}}\right|^2, \tag{11.3}$$

where f_{PP}, g_{PP} are defined in (5.9). Using (11.3), the maximum absorbed power can be obtained as

$$P_{\max} = \frac{\left|q_D + q_R\right|^2}{8 \cdot f_{PP}} \tag{11.4}$$

corresponding to an optimum inner pressure head $p_{\text{in}0_{\text{opt}}}$, equal to

$$p_{\text{in}0_{\text{opt}}} = \frac{q_D + q_R}{2 \cdot f_{PP}}. \tag{11.5}$$

The capture width ℓ [7, 11] is the ratio of the power absorbed by the device to the available power per unit crest length of the incident wave, that is,

$$\ell = \frac{2 \cdot P_{\text{out}}}{\rho \cdot g \cdot (H/2)^2 \cdot C_g}. \tag{11.6}$$

where C_g is the group velocity of the incident wave, given by

$$C_g = \frac{1}{2}\frac{\omega}{k}\left(1 + \frac{2kd}{\sinh(2kd)}\right), \tag{11.7}$$

and k is the wave number.

In order to achieve maximum capture width, it is not always practical to change the device's geometry, but it is likely easier to control the rotational speed N and the turbines diameter D. The optimum value of g_T, (5.17), is obtained from $\partial\ell/\partial g_T = 0$ and from (11.6) it is equal to

$$g_{T_{\text{opt}}} = \sqrt{f_{PP}^2 + \left(g_{PP} + \frac{\omega V_0}{\gamma P_a}\right)^2}. \tag{11.8}$$

When g_T takes the above optimum value, the maximum value of the absorbed power can be written in the bellow form:

$$P_{\max} = \frac{\left|q_D + q_R\right|^2}{8 \cdot f_{PP}}\left\{1 - \frac{2 \cdot g_{T_{\text{opt}}} \cdot \left(g_{T_{\text{opt}}} - f_{PP}\right)}{2 \cdot g_{T_{\text{opt}}} \cdot \left(g_{T_{\text{opt}}} + f_{PP}\right) - 4 \cdot \dfrac{\omega V_0}{\gamma P_a} \cdot g_{PP}}\right\}. \tag{11.9}$$
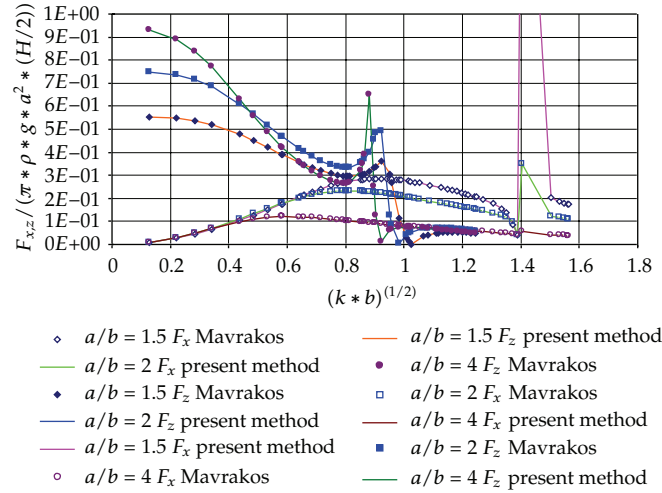
Figure 2: Horizontal and vertical exciting force on the OWC device for different cases of wall thickness.

12. Numerical Results

The calculation of the Fourier coefficients $F^I_{j,m,i}$, $F^{III}_{j,m,n}$, $F^{*III}_{j,m,n}$, $F^M_{j,m,i}$, $j = D, 1, 3, 5$, and P is the most significant part of the numerical procedure, because of their influence on the accuracy of solution. For the case of the first and the Mth ring element, $i = 20$, terms were used, while for the third ring element $N = 50$, since it was found that the results obtained for those values were correct to an accuracy of within 1%.

Since the pressure contribution inside the chamber affects only the vertical forces exerted on the device, the horizontal exciting force coincides with the one computed by Mavrakos [16] for a device open to the atmosphere. So, at first for the sake of computer code's verification, a geometric configuration investigated in [16] has been chosen. It is a body with immersion $h/b = 3.46$ and water depth $d/b = 4$ for three cases of wall thickness $a/b = 4$, $a/b = 2$, and $a/b = 1.5$. In Figure 2 the horizontal and vertical exciting force on the OWC device is compared with the results by Mavrakos [16] for the moon pool body when the inner pressure is equal to the atmospheric.

Then, a three-dimensional oscillating water column device is investigated, which is floating in a water depth $d = 15$ m with chamber's draught equal to 5 m. The OWC's internal and external radii are 2 m and 4 m, respectively. The vertical force on the restrained device due to a unit inner pressure head, expressed though (6.5), is plotted in Figure 3.

Next, we examine how the results' accuracy is affected by the number of terms considered in the potentials' series expansions. In Figures 4 and 5 the values of $f_{x_N} - f_{x_{10}}/f_{x_{10}}$ and $f_{z_N} - f_{z_{10}}/f_{z_{10}}$ are plotted for various numbers of series terms N. Here, f_{x_N} and f_{z_N} are the modulus of the horizontal and the total vertical exciting force, respectively, exerted on the same as the above OWC device with a turbine parameter $g_T = 1 \text{ m}^5/(\text{N·s})$.

In Tables 1 and 2, the module of the air pressure trapped in the OWC chamber is presented for the various values of g_T and ka. The same geometry of the OWC is assumed as the one previously examined. In Table 1 results for the restrained device, while in Table 2 for the free floating one, are given. It is worthwhile to mention that when $g_T \gg 0$, the device's chamber is approximating the open condition, so the inner pressure head tends to zero. On
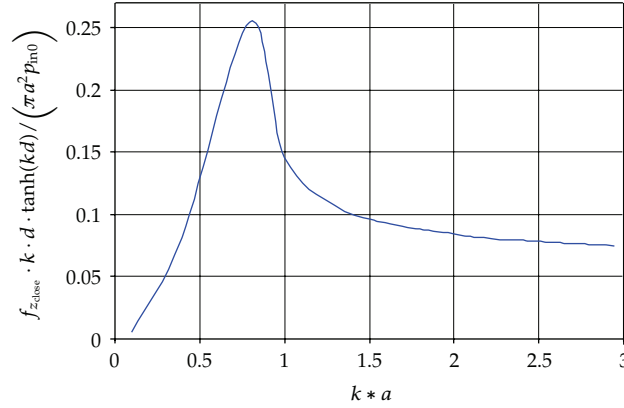
Figure 3: Vertical exciting force on the OWC device due to a unit inner pressure head.
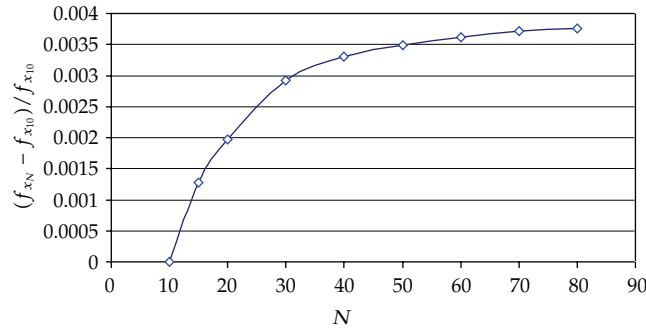
Figure 4: Graphics for $f_{x_N} - f_{x_{10}}/f_{x_{10}}$ versus N element terms.

the contrary, by letting $g_T \rightarrow 0$ the turbine at the top of the chamber is approximating the closed condition, thus the air chamber pressure is increased.

Next, comparisons are presented with the results given by Martins-Rivas and Mei [11]. To this end, we assume a vertical cylindrical oscillating water column device, having a wall thickness $(a - b)/d = 0.005$, external radius $a/d = 0.5$ and floating with a draught $(d - h)/d = 0.2$. Figure 6 concerns the conductance, B, and susceptance, C, as defined by $B = \text{Re}[(q_p/p_{in0})/(a/\omega\rho)]$ and $C = \text{Im}[(q_p/p_{in0})/(a/\omega\rho)]$, respectively, while in Figure 7 the nondimensional optimum turbine parameter $g_T \cdot \rho/a$ is plotted against the wave number parameter kd. In calculating the optimum turbine parameter though (11.8) since isentropy is assumed $\gamma P_a = c_a^2$, c_a being the sound velocity in air. The comparisons with the results of Martins-Rivas and Mei [11] are excellent.

Next, in Table 3 the RAOs of the heave motion are given against $\omega^2 b/g$ for an OWC device with dimensions $d/b = 2$, $d - h/b = 1/3$ and $a/b = 1.8$, $a/b = 1.2$, and $a/b = 1.034$. The results are compared with those by Mavrakos and Bardis [29] that correspond to the open moon pool case. For the present calculations, a value of $g_T = 1000 \, \text{m}^5/(\text{N·s})$ is assumed in order to approximate the open chamber case.
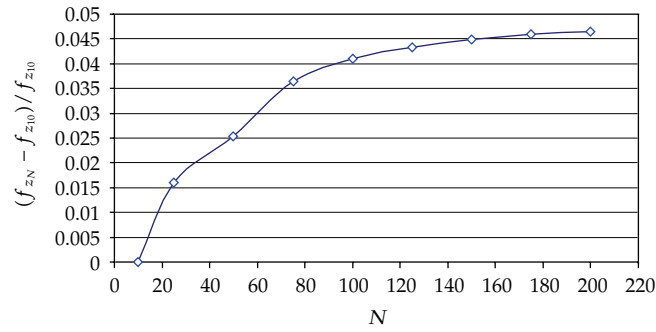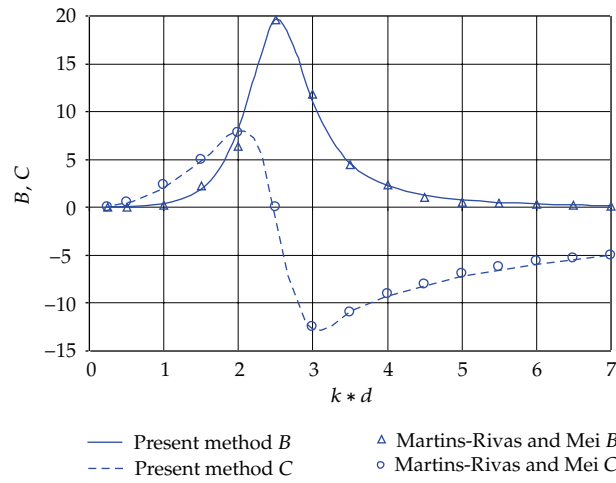
Further comparisons concerning the free surface elevation inside and outside of the device are presented in Figures 8 and 9 when $g_T \gg 0$. The results are compared to those of Mavrakos [16] for an open moonpool cylinder. The device's immersion is $h = 10 \, \text{m}$, inner

Table 1: Modulus of the inner pressure $p_{in0}/(H/2)$ for various values of g_T and ka, for a restrained OWC device.

	$g_T = 0.5$	$g_T = 1$	$g_T = 2$	$g_T = 3$	$g_T = 6$	$g_T = 10$
$k \cdot a = 0.4$	$4.94E + 00$	$4.71E + 00$	$4.05E + 00$	$3.39E + 00$	$2.11E + 00$	$1.35E + 00$
$k \cdot a = 1.0$	$1.30E + 00$	$1.26E + 00$	$1.12E + 00$	$9.71E - 01$	$6.33E - 01$	$4.15E - 01$
$k \cdot a = 1.5$	$4.85E - 01$	$4.36E - 01$	$3.30E - 01$	$2.50E - 01$	$1.39E - 01$	$8.60E - 02$
$k \cdot a = 2.0$	$1.93E - 01$	$1.62E - 01$	$1.11E - 01$	$7.98E - 02$	$4.24E - 02$	$2.61E - 02$

Table 2: Modulus of the inner pressure $p_{in0}/(H/2)$ for various values of g_T and ka, for a floating OWC device with mass moment of inertia $I = 1738.87\,\text{tn} \cdot \text{m}^2$.

	$g_T = 0.5$	$g_T = 1$	$g_T = 2$	$g_T = 3$	$g_T = 6$	$g_T = 10$
$k \cdot a = 0.4$	$5.87E - 01$	$5.68E - 01$	$5.07E - 01$	$4.38E - 01$	$2.85E - 01$	$1.85E - 01$
$k \cdot a = 1.0$	$4.02E - 01$	$3.98E - 01$	$3.84E - 01$	$3.63E - 01$	$2.82E - 01$	$2.13E - 01$
$k \cdot a = 1.5$	$1.52E - 01$	$1.45E - 01$	$1.26E - 01$	$1.06E - 01$	$6.37E - 02$	$4.18E - 02$
$k \cdot a = 2.0$	$6.73E - 02$	$6.21E - 02$	$4.91E - 02$	$3.86E - 02$	$2.13E - 02$	$1.36E - 02$

Figure 5: Graphics for $f_{z_N} - f_{z_{10}}/f_{z_{10}}$ versus N element terms.

Present method B
Present method C
△ Martins-Rivas and Mei B
○ Martins-Rivas and Mei C

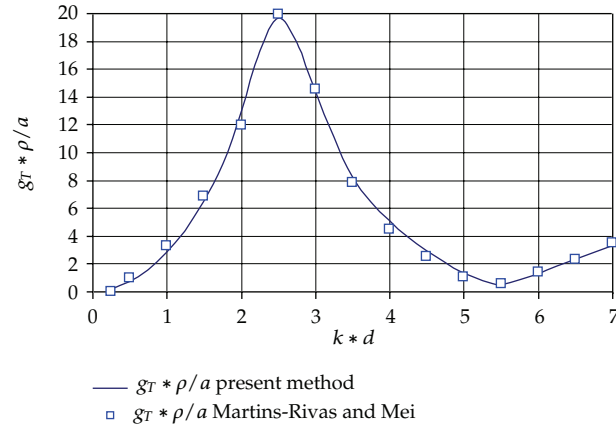**Figure 6:** Conductance B and susceptance C for an isolated OWC device in the open sea.

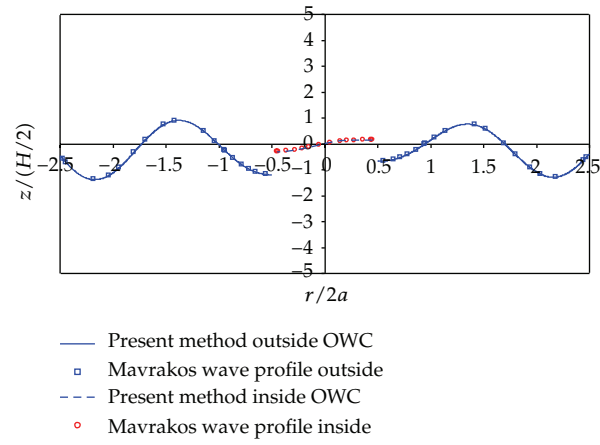**Figure 7:** Optimum turbine parameter admittance $g_T \cdot (\rho/a)$ versus kd.

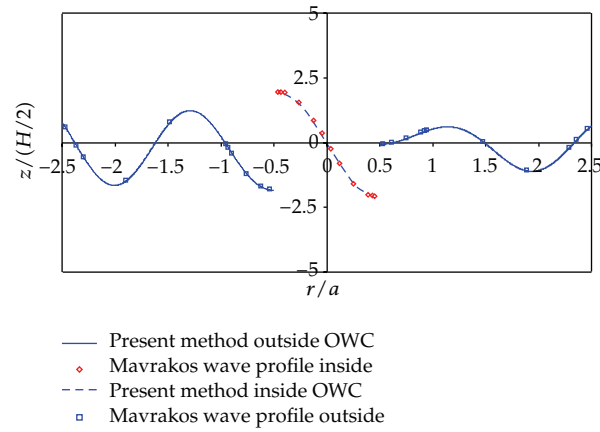**Figure 8:** Wave profile inside and outside OWC device for a wave period $T = 6.3\,\mathrm{s}$.

Figure 9: Wave profile inside and outside OWC device for a wave period $T = 6.0\,\mathrm{s}$.
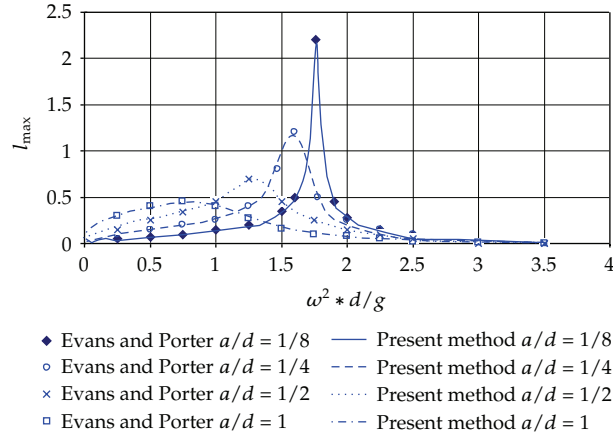
Figure 10: The maximum capture width against $\omega^2 \cdot d/g$ in various geometries of a restrained OWC device.
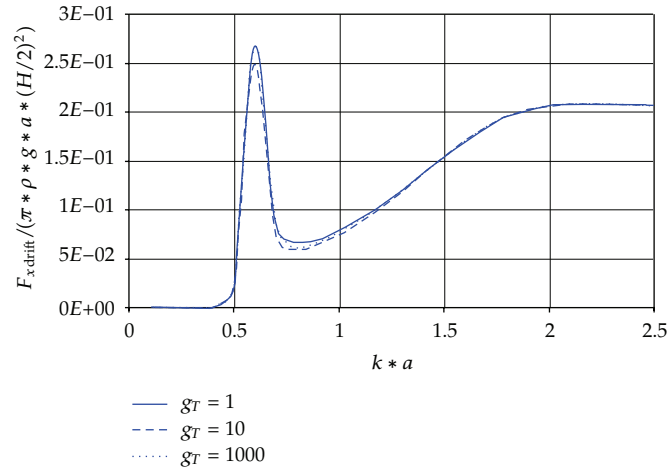

Figure 11: Horizontal mean second-order wave drift forces against $k \cdot a$ for various turbine parameters $g_T = 1, 10, 1000 \ (\mathrm{m}^5/(\mathrm{N \cdot s}))$.

and outer radius are $b = 2\,\mathrm{m}$, $a = 20\,\mathrm{m}$, respectively, and the water depth is $d = 20\,\mathrm{m}$. In Figures 8 and 9 the wave profile inside and outside of the structure is being presented for wave periods $T = 6.3\,\mathrm{s}$ and $T = 6.0\,\mathrm{s}$, wave lengths $\lambda = 59.8\,\mathrm{m}$ and $\lambda = 54.8\,\mathrm{m}$, respectively, and $g_T = 100\,\mathrm{m}^5/(\mathrm{N \cdot s})$. The angle of wave attack is $\theta = 0°$.

Next, the OWC device examined in Figure 3 is further investigated here with the aid of Table 4 as far the wave runup (see (9.2) and (9.1)) inside and outside the structure is concerned. For the calculations three values of turbine parameter $\Lambda = g_T = 1, 10, 100$ $(\mathrm{m}^5/(\mathrm{N \cdot s}))$ are assumed for $t = 0\,\mathrm{s}$.

We can observe that the wave runup on the structure's external wall tends to almost the same values independent of whether the duct is closed or open to the atmosphere (expressed though the various g_T values of turbine parameters; values of g_T tending to zero correspond to almost closed chamber, while large values to the open duct case). Contrary, the wave runup on the inner wall is affected by the g_T values.

Table 3: RAOs of heave motion $x_{30}/(H/2)$ versus $\omega^2 b/g$ for a floating OWC device with turbine parameter $g_T = 1000 \, \text{m}^5/(\text{N} \cdot \text{s})$. Comparisons with an open moon pool cylinder.

$\omega^2 b/g$	Open moon pool cylinder [29]			OWC device with $g_T = 1000 \, \text{m}^5/(\text{N} \cdot \text{s})$		
	$a/b = 1.8$	$a/b = 1.2$	$a/b = 1.034$	$a/b = 1.8$	$a/b = 1.2$	$a/b = 1.034$
0.037	0.9549	0.9733	0.9716	0.9548	0.9733	0.9718
0.883	0.6458	0.9582	0.9462	0.6440	0.9576	0.9489
1.223	0.0124	0.5061	0.7706	0.0191	0.5038	0.7864
1.348	0.2244	0.2075	0.5358	0.2201	0.2094	0.5665
1.761	0.6407	0.3720	0.1550	0.6118	0.3639	0.2022
1.926	0.3234	0.6149	0.2998	0.3196	0.5862	0.3011

Table 4: Wave runup inside and outside an OWC device versus ka. Angle of wave attack $\vartheta = 0$.

$k \cdot a$	Wave runup on the outer OWC's surface			Wave runup on the inner OWC's surface		
	$g_T = 1$	$g_T = 10$	$g_T = 100$	$g_T = 1$	$g_T = 10$	$g_T = 100$
0.4	0.8313	0.8305	0.8313	1.5166	1.6172	1.6361
0.8	0.3555	0.3507	0.3502	−0.4638	−0.4492	−0.0742
1.0	0.0825	0.0811	0.0821	−0.1741	−0.1374	−0.0988
1.3	−0.4048	−0.4061	−0.4049	−0.0814	−0.0691	−0.0622
1.6	−0.8494	−0.8507	−0.8494	−0.0807	−0.0765	−0.0740
2.0	−1.3019	−1.3029	−1.3019	−0.1256	−0.1249	−0.1238

The maximum absorbed energy (see (11.4)) for the same as the above OWC device is presented in Table 5 versus ka.

Next, in Figure 10 the maximum capture width is plotted for a restrained OWC device with various external radius to water depth ratios $a/d = 1/8, 1/4, 1/2$, and 1, wall thickness $(a - b)/d = 0.005$, and floating in a water depth $d/h = 2$. These results are compared very well with the ones given in Evans and Porter [7] work.

Finally, in Figure 11 results concerning the horizontal mean second-order wave drift forces exerted on the OWC device that was investigated in Figure 3 of the present work are given for three different values of the turbine admittance characteristics g_T.

13. Conclusion

An analytical method has been developed to solve the diffraction and radiation problems around a floating vertical axisymmetric OWC device. This method provides an efficient tool for the complete hydrodynamic analysis of this important type of wave energy conversion devices, including the evaluation of the first-order wave exciting forces, the mean second-order wave drift forces, the hydrodynamic parameters, the pressure head inside the chamber, the air flow flux, and the maximum absorbed power. The results of this analysis are of particular importance for the design of such types of wave energy converters, for which the hydrodynamic parameters and the turbine characteristics have to be combined in order to improve the wave energy conversion.

Table 5: Comparison between the maximum energy $P_{\max}/(H/2)^2$ of a restrained and a floating OWC device versus ka. The mass moment of inertia $I = 1738.87\,\text{tn} \cdot \text{m}^2$.

$k \cdot a$	Restrained OWC device	Floating OWC device
0.2	956.983	0.3219
0.4	308.105	5.7967
0.6	147.688	139.779
0.8	90.6602	31.8176
1.0	63.7096	16.7789
1.5	34.5299	8.1777
2.0	22.5046	6.1624
2.5	16.1687	5.2424
3.0	12.3529	4.6839

Appendices

A. Values of the Coefficients $L_{q,i}$

The defining equations for $L_{q,j}$ are (4.1), (4.2), (4.5), and (4.6).

One has

$$L_{q,i} = \frac{1}{h}\int_0^h Z_i(z)\cos\left(\frac{q\pi z}{h}\right)dz = (-1)^q\left[\frac{1}{2}\left[1+\frac{\sin(2a_i d)}{2a_i d}\right]\right]^{-1/2}\frac{a_i h}{a_i^2 h^2 - q^2\pi^2}\sin(a_i h), \quad \text{(A.1)}$$

when $i \geq 1$, $a_i \neq q\pi/h$

$$L_{q,0} = (-1)^q\left[\frac{1}{2}\left[1+\frac{\sinh(2kd)}{2kd}\right]\right]^{-1/2}\frac{kh}{k^2 h^2 + q^2\pi^2}\sinh(kh), \quad \text{(A.2)}$$

when $i = 0$

$$L_{q,i} = \frac{1}{2}\left[\frac{1}{2}\left[1+\frac{\sin(2a_i d)}{2a_i d}\right]\right]^{-1/2} \quad \text{(A.3)}$$

when $i \geq 1$, $a_i = q\pi/h \neq 0$.

Values of $Q_{P,0,q}^*$ (see (4.4))

$$Q_{P,0,q}^* = \begin{cases} 0, & q \neq 0, \\ 1, & q = 0. \end{cases} \quad \text{(A.4)}$$

B. Matrix of the Body's Rotational Motions and Relative Wave Height Elevation

For the description of the fluid flow around the floating OWC device, an inertial cylindrical coordinate system (r, θ, z) with origin on the sea bottom (see Figure 1) has been used. Next, in order to describe the kinematics of a point on the instantaneous wetted surface of the

body, as it is required for the wave drift forces calculations, see (10.1) and (10.2), a body-fixed coordinate system $G - xyz$ with origin at the body's centre of gravity, G, is additionally introduced. The surface of the body is defined relative to this system of axes and a point on the surface has as a position the vector $\bar{x}$. The matrix of first-order rotations R in (10.1) and (10.2) is given by

$$R = \begin{bmatrix} 0 & -x_6 & x_5 \\ x_6 & 0 & -x_4 \\ -x_5 & x_4 & 0 \end{bmatrix} \tag{B.1}$$

and the acceleration matrix for the body's centre of gravity $\ddot{X}_g$ is

$$\overline{\ddot{X}_g} = \begin{bmatrix} -\omega^2 \cdot x_1 \\ 0 \\ -\omega^2 \cdot x_3 \end{bmatrix}. \tag{B.2}$$

The relative wave height in (10.1) is equal to

$$\zeta_r = \zeta - x_{3WL} = -\frac{1}{g} \frac{\partial \Phi}{\partial t} - (x_3 - x_5 \cdot r \cdot \cos \theta) \tag{B.3}$$

and the displacement vector of a point on the device, $\overline{X}$, is

$$\overline{X} = \overline{X_g} + R \cdot \overline{x}. \tag{B.4}$$

Acknowledgments

References

[1] A. Clément, P. McCullen, A. Falcão et al., "Wave energy in Europe: current status and perspectives," *Renewable and Sustainable Energy Reviews*, vol. 6, no. 5, pp. 405–431, 2002.

[2] A. F. D. O. Falcão, "Wave energy utilization: a review of the technologies," *Renewable and Sustainable Energy Reviews*, vol. 14, no. 3, pp. 899–918, 2010.

[3] M. E. McCormick, "Analysis of a wave energy conversion buoy," *Journal of Hydronautics*, vol. 8, no. 3, pp. 77–82, 1974.

[4] M. E. McCormick, "A modified linear analysis of a wave-energy conversion buoy," *Ocean Engineering*, vol. 3, no. 3, pp. 133–144, 1976.

[5] D. V. Evans, "Wave-power absorption by systems of oscillating surface pressure distributions," *Journal of Fluid Mechanics*, vol. 114, pp. 481–499, 1982.

[6] A. J. N. A. Sarmento, L. M. C. Gato, and A. F. D. O. Falcão, "Turbine-controlled wave energy absorption by oscillating water column devices," *Ocean Engineering*, vol. 17, no. 5, pp. 481–497, 1990.

[7] D. V. Evans and R. Porter, "Efficient calculation of hydrodynamic properties of OWC-type devices," *Journal of Offshore Mechanics and Arctic Engineering*, vol. 119, no. 4, pp. 210–218, 1997.

[8] K. Kokkinowrachos, I. Thanos, and H. G. Zibell, "Hydrodynamic analysis of some wave energy conversion systems," in *Proceedings of the OCEANS'87 Conference*, pp. 566–574, Halifax, Canada, September 1987.

[9] Y. Masuda, "Wave-activated generator," in *Proceedings of the International Colloquium on the Exposition of the Oceans*, Boudreaux, France, 1971.

[10] Y. Masuda, "Experimental full-scale results of wave power machine Kaimei in 1978," in *Proceedings of the 1st Symposium on Wave Energy Utilization*, pp. 349–363, Gothenburgh, Sweden, 1979.

[11] H. Martins-Rivas and C. C. Mei, "Wave power extraction from an oscillating water column at the tip of a breakwater," *Journal of Fluid Mechanics*, vol. 626, pp. 395–414, 2009.

[12] A. F. O. Falcão, J. C. C. Henriques, and J. J. Cândido, "Dynamics and optimization of the OWC spar buoy wave energy converter," *Renewable Energy*, vol. 48, pp. 369–381, 2012.

[13] J. Miles and F. Gilbert, "Scattering of gravity waves by a circular dock," *Journal of Fluid Mechanics*, vol. 34, no. 4, pp. 783–793, 1968.

[14] C. J. R. Garrett, "Wave forces on a circular dock," *The Journal of Fluid Mechanics*, vol. 46, no. 1, pp. 129–139, 1971.

[15] R. W. Yeung, "Added mass and damping of a vertical cylinder in finite-depth waters," *Applied Ocean Research*, vol. 3, no. 3, pp. 119–133, 1981.

[16] S. A. Mavrakos, "Wave loads on a stationary floating bottomless cylindrical body with finite wall thickness," *Applied Ocean Research*, vol. 7, no. 4, pp. 213–224, 1985.

[17] S. A. Mavrakos, "Hydrodynamic coefficients for a thick-walled bottomless cylindrical body floating in water of finite depth," *Ocean Engineering*, vol. 15, no. 3, pp. 213–229, 1988.

[18] K. Kokkinowrachos, S. Mavrakos, and S. Asorakos, "Behaviour of vertical bodies of revolution in waves," *Ocean Engineering*, vol. 13, no. 6, pp. 505–538, 1986.

[19] T. Setoguchi and M. Takao, "Current status of self rectifying air turbines for wave energy conversion," *Energy Conversion and Management*, vol. 47, no. 15-16, pp. 2382–2396, 2006.

[20] R. Curran and M. Folley, "Air turbine design for OWCs," in *Ocean Wave Energy*, J. Cruz, Ed., pp. 189–219, Springer, Berlin, Germany, 2008.

[21] C. C. Mei, *The Applied Dynamics of Ocean Surface Waves*, John Wiley & Sons, New York, NY, USA, 1983.

[22] J. Falnes, *Ocean Waves and Oscillating Systems: Linear Interactions Including Wave-Energy Extraction*, Cambridge University Press, New York, NY, USA, 2002.

[23] A. F. D. O. Falcão and P. A. P. Justino, "OWC wave energy devices with air flow control," *Ocean Engineering*, vol. 26, no. 12, pp. 1275–1295, 1999.

[24] S. L. Dixon, *Fluid Mechanics, Thermodynamics of Turbomachinery*, Pergamon, Oxford, UK, 3rd edition, 1978.

[25] A. F. D. O. Falcão, "Control of an oscillating-water-column wave power plant for maximum energy production," *Applied Ocean Research*, vol. 24, no. 2, pp. 73–82, 2002.

[26] A. J. N. A. Sarmento and A. F. D. O. Falcão, "Wave generation by an oscillating surface-pressure and its application in wave-energy extraction," *Journal of Fluid Mechanics*, vol. 150, pp. 467–485, 1985.

[27] J. N. Newman, *Marine Hydrodynamics*, MIT Press, Cambridge, Mass, USA, 1977.

[28] J. A. Pinkster and G. van Oortmerssen, "Computation of the first and second order wave forces on oscillating bodies in regular waves," in *Proceedings of the 2nd International Conference on Numerical Ship Hydrodynamics*, pp. 136–159, Berkley, Mich, USA, 1977.

[29] S. A. Mavrakos and L. Bardis, "Hydrodynamic analysis of floating solar ponds," in *Proceedings of the Marine Computers'86*, pp. 24.1–24.12, The Society of Naval Architects and Marine Engineers (SNAME), MIT, Cambridge, Mass, USA, 1986, paper no. 24.